Bioconjugate Chemistry

Article

pubs.acs.org/bc

Rerouting the Metabolic Pathway of ^{18}F-Labeled Peptides: The Influence of Prosthetic Groups

Susan Richter,[†] Melinda Wuest,[†] Cody N. Bergman,[†] Jenilee D. Way,[†] Stephanie Krieger,[‡] Buck E. Rogers,[‡] and Frank Wuest*[,†]

[†]Department of Oncology, University of Alberta, Cross Cancer Institute, 11560 University Avenue, Edmonton, Alberta T6G 2X4, Canada

[‡]Department of Radiation Oncology, Washington University School of Medicine, 4511 Forest Park Boulevard, St. Louis, Missouri 63108, United States

Supporting Information

ABSTRACT: Current translational cancer research is directed to the development of high affinity peptide ligands for targeting neuropeptide receptors overexpressed in different types of cancer. Besides their desired high binding affinity to the receptor, the suitability of radiolabeled peptides as targeting vectors for molecular imaging and therapy depends on additional aspects such as high tumor-to-background ratio, favorable clearance pattern from nontarget tissue, and sufficient metabolic stability in vivo. This study reports how a switch from the prosthetic group, *N*-succinimidyl-4-[^{18}F]-fluorobenzoate ([^{18}F]SFB), to 2-deoxy-2-[^{18}F]fluoro-D-glucose ([^{18}F]FDG) effects the metabolic pathway of an ^{18}F-labeled bombesin derivative, QWAV-Sar-H-FA01010-Tle-NH$_2$. ^{18}F-Labeled bombesin derivatives represent potent peptide ligands for selective targeting of gastrin-releasing peptide (GRP) receptor-expressing prostate cancer. Radiosynthesis of ^{18}F-labeled bombesin analogues [^{18}F]**FBz-Ava-BBN2** and [^{18}F]**FDG-AOAc-BBN2** was achieved in good radiochemical yields of ∼50% at a specific activity exceeding 40 GBq/μmol. Both nonradioactive compounds **FBz-Ava-BBN2** and **FDG-AOAc-BBN2** inhibited binding of [^{125}I]Tyr^4-bombesin(1−14) in PC3 cells with IC$_{50}$ values of 9 and 16 nM, respectively, indicating high inhibitory potency. Influence of each prosthetic group was further investigated in PC3 mouse xenografts using dynamic small animal PET imaging. In comparison to [^{18}F]**FBz-Ava-BBN2**, total tumor uptake levels were doubled after injection of [^{18}F]**FDG-AOAc-BBN2** while renal elimination was increased. Blood clearance and in vivo metabolic stability were similar for both compounds. The switch from [^{18}F]SFB to [^{18}F]FDG as the prosthetic group led to a significant reduction in lipophilicity which resulted in more favorable renal clearance and increased tumor uptake. The presented single step radiolabeling-glycosylation approach represents an innovative strategy for site-directed peptide labeling with the short-lived positron emitter ^{18}F while providing a favorable pharmacokinetic profile of ^{18}F-labeled peptides.

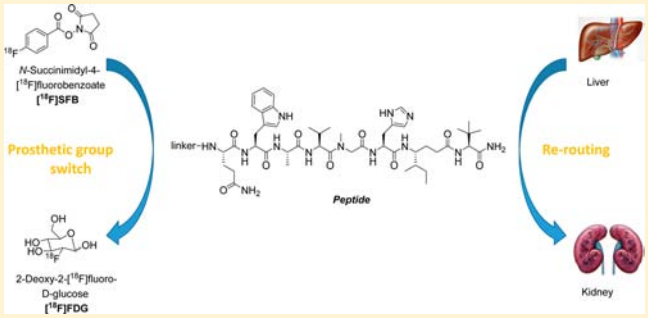

INTRODUCTION

Peptide receptor-based targeted molecular imaging and therapy of cancer is on the current forefront of nuclear medicine preclinical research and clinical practice.[1−6] The rationale behind the utilization of radiolabeled peptides for targeted molecular imaging and therapy is the frequent overexpression of several receptors for regulatory peptides on cellular membranes of tumor cells. Most of these receptors belong to the G-protein coupled receptor family. Prominent examples of radiolabeled peptides are somatostatin analogues, neurotensin derivatives, vasoactive intestinal peptides, and cholecystokinin analogues. Other important peptides for molecular imaging and therapy of cancer are radiolabeled bombesin derivatives. Bombesin-based peptides bind to gastrin-releasing peptide (GRP) receptors, which are members of the mammalian bombesin receptor family. GRP receptors also belong to the class of the 7-transmembrane G-protein-coupled receptors.[7] Elevated levels of GRP receptors are found in >60% of prostate cancer patients,[8,9] while only low or no expression is found for other bombesin receptor family members such as neuromedin B (NMB) receptor and BRS-3.[10] Moreover, elevated expression of GRP receptors was also reported in breast, pancreatic, and small-cell lung cancer.[11] Its potential as a suitable molecular target in cancer led to the design and development of cytotoxic and radiolabeled bombesin derivatives for molecular imaging, monitoring, and treatment of cancer.[3,11−14] Like all radiolabeled peptides for molecular imaging and therapy of cancer, radiolabeled bombesin derivatives have to meet several criteria to be useful as targeting vectors in nuclear medicine. These criteria include favorable tumor to nontarget ratios, sufficiently high metabolic stability, and favorable pharmacokinetic

Received: July 18, 2014
Published: January 9, 2015

DOI: 10.1021/bc500599m
Bioconjugate Chem. 2015, 26, 201−212

parameters with regard to clearance patterns from blood and nontumor tissues. All of these criteria are reflected by the metabolism of radiolabeled peptides. Optimization of metabolism of radiolabeled peptides for molecular imaging and therapy remains a special challenge.

In addition to the ongoing discussion regarding whether radiolabeled bombesin antagonists would be more favorable for GRP receptor targeting compared to bombesin agonists,[13−19] modification of the pharmacokinetic profile to enhance tumor uptake in vivo is the subject of intense research activity.[12,20] A major drawback of radiolabeled bombesin derivatives for targeting GRP receptors is their fairly high lipophilicity resulting in substantial clearance through the gastrointestinal tract, and some limitations emerge from the detection of metastatic lesions of prostate cancer, e.g., in the liver.[21] Thus, radiolabeled bombesin derivatives should preferentially display low hepatic uptake.[22]

Toward this goal, Waengler and Schirrmacher[23] have introduced sugar moieties, negatively charged carboxylic or sulfonic acids, and positively charged quarternary ammonium groups into the ^{18}F-SiFA-labeled PEGylated bombesin derivative PESIN (a PEG_4 motif-bearing native bombesin(7−14) labeled with an ^{18}F-silicon-fluoride-acceptor building block at the *N*-terminus) to lower lipophilicity and to improve the pharmacokinetic profile. This approach reduced lipophilicity expressed as $logD_{7.4}$ (*n*-octanol/PBS) from +2.29 to −1.22 while receptor binding affinities remained almost unchanged. However, favorable GRP receptor imaging in PC3 tumors was limited by high background activity.[23]

Modification of the pharmacokinetic profile of radiolabeled peptides can be achieved by the introduction of sugar moieties into the peptide backbone. Based on this concept, Wester et al. have studied several ^{125}I-labeled and ^{18}F-fluoropropionyl (FP)-labeled glycosylated octreotide and octreotate derivatives for somatostatin receptor targeting in neuroendocrine tumors. They found that peptide carbohydration did not change receptor affinity, but reduced lipophilicity and decreased overall intestinal radioactivity.[24] The carbohydrated octreotate derivative Gluc-Lys-([^{18}F]FP)-TOCA displayed an excellent pharmacokinetic profile as an imaging agent characterized by a high tumor to nontarget ratio, low uptake levels in the liver, and rapid urinary excretion.[25] Another prominent example of glycosylated radiolabeled peptides is galactose-containing cyclic RGD peptide [^{18}F]Galacto-RGD targeting $\alpha_v\beta_3$ integrins. [^{18}F]Galacto-RGD is among the most studied ^{18}F-labeled peptides in the clinic so far.[26,27] All of these radiolabeled glycopeptides were synthesized starting from glycosylated peptides as a labeling precursor through bioconjugation using prosthetic groups[24−27] or ^{19}F/^{18}F isotopic exchange reaction.[23]

The present study suggests glycosylation of ^{18}F-labeled peptides via a simplified strategy combining glycosylation and radiolabeling in a single step. [^{18}F]FDG has recently been described as a prosthetic group for peptide labeling with ^{18}F.[28,29]

This study describes the synthesis and radiopharmacological evaluation of ^{18}F-radiolabeled bombesin derivatives for targeting GRP receptors in prostate cancer. Prosthetic groups [^{18}F]SFB and [^{18}F]FDG are used for radiolabeling the bombesin derivative, QWAV-Sar-H-FA01010-Tle-NH_2, with ^{18}F. Radiopharmacological evaluation in GRP receptor-expressing PC3 mouse xenografts is focused on the analysis of different elimination pathways with regard to more renal excretion (rerouting) depending on the selected prosthetic group.

RESULTS AND DISCUSSION

The concept of rerouting the metabolic pathway of radiolabeled peptides was studied using two metabolically stabilized derivatives based on native bombesin(7−14). Positions 11, 13, and 14 of bombesin(7−14) were substituted with *N*-methyl-glycine (Sar), (4*S*,5*R*)-4-amino-5-methyl-heptanoic acid (FA01010), and *tert*-leucine (Tle) to reduce degradation through ubiquitously present peptidases in vivo.[30,31] 5-Amino-valeric acid (Ava) was introduced as a linker between the *N*-terminal end of the peptide backbone and the acylation site for [^{18}F]SFB labeling to provide ^{18}F-labeled peptide [^{18}F]**FBz-Ava-BBN2**.[32] The physicochemical properties of [^{18}F]**FBz-Ava-BBN2** are characterized by a fairly high lipophilicity as expressed by a logP value of 1.2. The hydrophobic nature of peptide [^{18}F]**FBz-Ava-BBN2** is based on by lipophilic amino acids in the peptide backbone such as Trp, Ala, Val, Tle, and FA01010.

In order to achieve a shift toward a more hydrophilic peptide, modification of the peptide backbone via glycosylation represents a viable option. For this purpose, the radiolabeled glucose analogue [^{18}F]FDG was selected as a prosthetic group. [^{18}F]FDG as the most important radiopharmaceutical for PET imaging is easily available in most PET centers worldwide. ^{18}F-Radiolabeling reactions with [^{18}F]FDG requires the presence of an amino-oxy group to form the corresponding oxime compounds. GRP-receptor binding peptide QWAV-Sar-H-FA01010-Tle-NH_2 was functionalized with an amino-oxy group through acylation reaction with 2-(aminooxy)acetic acid. Chemical yields of peptides **Ava-BBN2** and **AOAc-BBN2** as labeling precursors with [^{18}F]SFB and [^{18}F]FDG were in the range of 27−30%. The reference compound **FBz-Ava-BBN2** was prepared on-resin through coupling 4-fluoro-benzoic acid to **Ava-BBN2**. **FBz-Ava-BBN2** was prepared in isolated chemical yields of 17% after cleavage from the resin, purification by HPLC, and lyophilization. The reference compound **FDG-AOAc-BBN2** was prepared in a combination of solid-phase synthesis and in-solution coupling. Chemical yields of **AOAc-BBN2** were in the range of 22−30% after cleavage, HPLC purification, and lyophilization. Modification with FDG in MeOH was obtained in-solution quantitatively. Peptide structures, obtained overall chemical yields, and ESI-MS data for characterization of reference compounds **FDG-AOAc-BBN2** and **FBz-Ava-BBN2** are summarized in Table 1.

In addition, Table 1 also shows IC_{50} values determined for reference compounds **FDG-AOAc-BBN2** and **FBz-Ava-BBN2** representing their inhibitory potency toward the GRP receptor.

Both peptides were tested in a competitive binding assay using prostate cancer cell line PC3 to analyze their potency to inhibit binding of [^{125}I]Tyr^4-bombesin(1−14) as tracer and internal reference to GRP receptors. The following concentrations for half-maximum inhibition (IC_{50}) were determined: 16.5 ± 1.3 nM (n = 3) for **FDG-AOAc-BBN2** and 8.7 ± 2.2 nM (n = 3) for **FBz-Ava-BBN2** as derived from the characteristic sigmoidal concentration−response curves (Figure 1). Introduction of FDG into bombesin derivative **AOAc-BBN2** resulted in a slightly reduced inhibitory potency compared to [^{18}F]SFB-modified bombesin derivative **FBz-Ava-BBN2**.[32] Internal reference compound I-Tyr^4-bombesin-(1−14) had an IC_{50} value of 3 nM, which confirms that both peptides **FDG-AOAc-BBN2** and **FBz-Ava-BBN2** possess an

DOI: 10.1021/bc500599m
Bioconjugate Chem. 2015, 26, 201−212

Table 1. Characterization of Stabilized Bombesin Peptides and Synthesis Parameters of ^{18}F-Labeled Counterparts

peptide	sequence[a]	synthesis yield	ESI-MS	IC_{50} value[b]	$logD_{7.4}$[b]	radiochemical yield[c]	A_S
FBz-Ava-BBN2	FBz-Ava-Q^{7}W^{8}A^{9}V^{10}-Sar^{11}-H^{12}-FA01010^{13}-Tle^{14}-NH$_2$	17%	1184.7 $[M + H]^+$	8.7 ± 2.2	+1.22 ± 0.02	52 ± 8%	≫40 GBq/μmol
FDG-AOAc-BBN2	FDG-AOAc-Q^{7}W^{8}A^{9}V^{10}-Sar^{11}-H^{12}-FA01010^{13}-Tle^{14}-NH$_2$	63%	1201.6 $[M + H]^+$ 601.3 $[M+2H]^{2+}$	16.5 ± 1.3	−0.73 ± 0.02	51 ± 24%	≫40 GBq/μmol

[a]Natural amino acids are expressed as one-letter-code. FBz = 4-fluorobenzoyl, Ava = 5-aminovaleric acid, Sar = sarcosine, *N*-methyl-glycine, FA01010 = (4*R*,5*S*)-4-amino-5-methylheptanoic acid, Tle = *tert*-leucine, FDG = 2-deoxy-2-fluoro-D-glucose, AOAc = aminooxy-acetic acid. [b]Data as mean ± SEM from n = 3 experiments. [c]Decay-corrected. n = 15 for [^{18}F]**FBz-Ava-BBN2**. n = 10 for [^{18}F]**FDG-AOAc-BBN2**.

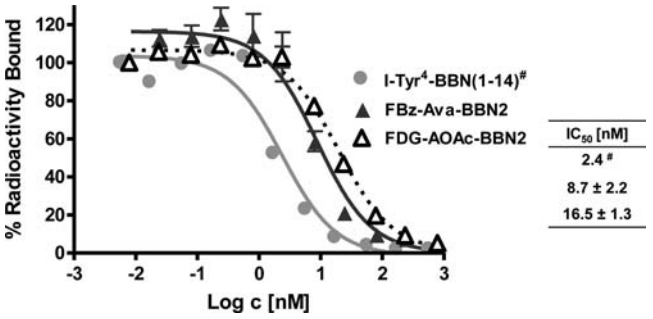

Figure 1. Concentration−response curve for the competitive binding assay. Determination of IC_{50} values for FBz-Ava-BBN2 and FDG-AOAc-BBN2 against ^{125}I-Tyr^4-bombesin(1−14) (pGlu-QR-[^{125}I]Tyr-GNQWAVGHLM-NH_2) binding to GRPR. Data as mean ± SEM from n = 3 triplicate experiments. # see ref 32.

inhibitory potency in a comparable concentration range. Therefore, glycosylation with FDG as a structural modification of the bombesin backbone seems not to interfere significantly with the binding to the GRP receptor.

Scheme 1 summarizes the ^{18}F-radiolabeling of the stabilized bombesin derivatives **Ava-BBN2** and **AOAc-BBN2** using prosthetic groups [^{18}F]SFB and [^{18}F]FDG including the reaction conditions used.

The radiolabeling reaction with [^{18}F]SFB as the prosthetic group was improved in comparison to our previously reported results.[32] The amount of precursor peptide **Ava-BBN2** as labeling precursor was reduced from 1 to 0.5 mg, and radiolabeling was carried out in 50 mM Na_2HPO_4 buffer (pH 9) providing 83% of fluorobenzoylated bombesin derivative [^{18}F]**FBz-Ava-BBN2** after a reaction time of 30 min at 40 °C. Based on these reaction conditions, the total isolated radiochemical yields could be increased to 52 ± 8% (n = 15). The radiochemical purity was greater than 95%, and specific activity was also increased, exceeding 40 GBq/μmol.

No nonradioactive **FBz-Ava-BBN2** was found in the quality control HPLC UV trace, and the labeling precursor **Ava-BBN2** could be removed completely by semipreparative HPLC.

Glycosylation of stabilized bombesin derivative **AOAc-BBN2** was achieved by oxime formation using a clinical batch of [^{18}F]FDG as a prosthetic group. [^{18}F]FDG has been introduced as a suitable prosthetic group for various peptide labeling experiments with ^{18}F.[28,29,33,34] Site-specific labeling was enabled through oxime formation between the *N*-terminal aminooxy group present in the labeling precursor **AOAc-BBN2** and the aldehyde group found in the open-chain form of [^{18}F]FDG. However, this reaction is somehow hampered and inefficient due to the fact that [^{18}F]FDG in solution exists mainly in its pyranose form rather than the reactive open chain aldehyde form. However, promotion of this type of condensation reaction can be reached by using aniline as a nucleophilic catalyst which forms an intermediate Schiff base product with [^{18}F]FDG as the more reactive species for the subsequent oxime formation.[34] Hence, transimination becomes the rate-determining step accelerating the whole reaction.[35] In a representative set of experiments, 500 μg of **AOAc-BBN2** dissolved in methanol−aniline solutions was reacted with [^{18}F]FDG in saline. Despite the presence of competing hexose D-glucose in the [^{18}F]FDG solution as typical for clinical [^{18}F]FDG batches, 60−80% of ^{18}F-gycosylated bombesin [^{18}F]**FDG-AOAc-BBN2** was found in the reaction mixture after 45 min at 85 °C. A further increase in the amount of

DOI: 10.1021/bc500599m
Bioconjugate Chem. 2015, 26, 201−212

Scheme 1. Radiolabeling of Stabilized Bombesin Peptides Ava-BBN2 and AOAc-BBN2 Using [^{18}F]SFB or [^{18}F]FDG as Prosthetic Groups

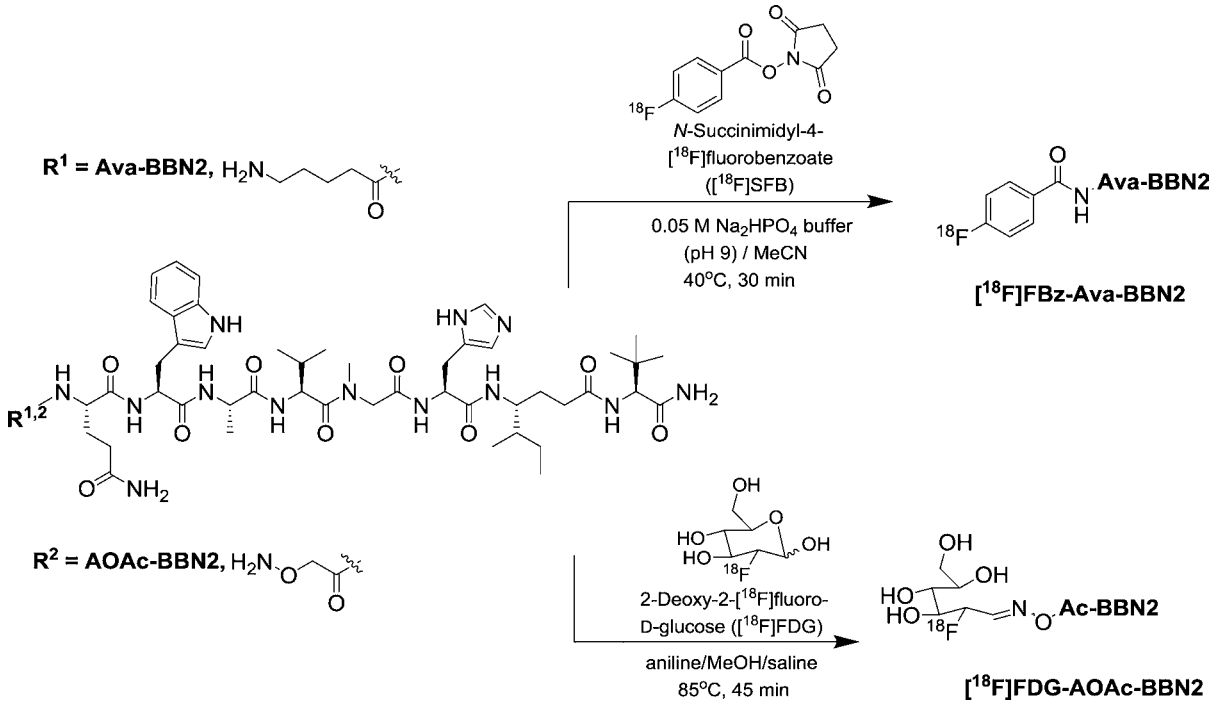

AOAc-BBN2 precursor from 500 μg to 700 μg resulted in a further increase of the oxime formation yield of up to 90−95%. High overall radiochemical yields of 51 ± 24% (n = 10) were achieved for [^{18}F]**FDG-AOAc-BBN2** after HPLC purification with radiochemical purities greater 99%. In contrast to Hultsch et al.,[33] no HPLC purification of [^{18}F]FDG prior to its use was necessary, since D-glucose-modified **AOAc-BBN2** could easily be separated from [^{18}F]**FDG-AOAc-BBN2**. Therefore, specific activities exceeding >40 GBq/μmol were obtained. Detailed information on radiolabeling procedures including HPLC traces can be found in the Supporting Information.

The lipophilicity of radiotracers [^{18}F]**FBz-Ava-BBN2** and [^{18}F]**FDG-AOAc-BBN2** was determined and represents the partition coefficient of both radiotracers between n-octanol and PBS (pH 7.4). As expected, [^{18}F]**FDG-AOAc-BBN2** showed much better solubility in PBS as reflected by a negative log D value of −0.73 ± 0.02 (n = 3). In contrast, [^{18}F]**FBz-Ava-BBN2** is more lipophilic as reflected by the positive log D value of +1.22 ± 0.02 (n = 3; Table 1).

Both ^{18}F-labeled bombesin analogues [^{18}F]**FBz-Ava-BBN2** and [^{18}F]**FDG-AOAc-BBN2** were further analyzed in vivo to determine metabolic stability. Sufficient in vivo metabolic stability represents an important basic requirement for successful application of radiolabeled peptides for peptide-receptor targeted molecular imaging and therapy of cancer. Native regulatory peptides often suffer from a very short biological half-life of ≤2 min due to degradation by ubiquitously present peptidases. To date, there is only limited information available on the stability of ^{18}F-labeled bombesins and derivatives in vivo. The majority of articles describe applications of bombesin derivatives containing the native bombesin(7−14) sequence.[11] Stability of [^{18}F]**FDG-AOAc-BBN2** and [^{18}F]**FBz-Ava-BBN2** in vivo was analyzed over a time course of 60 min in murine blood samples. At 3, 10, 15, 30, 45, and 60 min p.i. of each radiotracer in normal BALB/c mice, blood samples were collected and processed by separation into blood cells, plasma proteins, and plasma fractions. Radioactivity distribution in all fractions was comparable for both radiolabeled peptides.

Binding to plasma proteins was found to be as high as 70% for both peptides after 5 min. Plasma protein binding dropped significantly over time reaching less than 10% after 60 min. This finding is indicative of good bioavailability of both radiolabeled peptides at later time points. After 60 min p.i., over 70% of intact [^{18}F]**FDG-AOAc-BBN2** and about 60−65% of intact [^{18}F]**FBz-Ava-BBN2** was found in the plasma fraction, leaving an average of 20−30% of bound radioactivity to blood cells. Plasma samples were analyzed with radio-HPLC to determine the amounts of intact ^{18}F-labeled bombesin derivatives.

Figure 2 summarizes in vivo metabolic stability results for [^{18}F]**FBz-Ava-BBN2** and [^{18}F]**FDG-AOAc-BBN2**, respectively.

Both ^{18}F-labeled bombesin derivatives remain mostly intact (>85%) over the first 10 min p.i.. Over the time course of 60

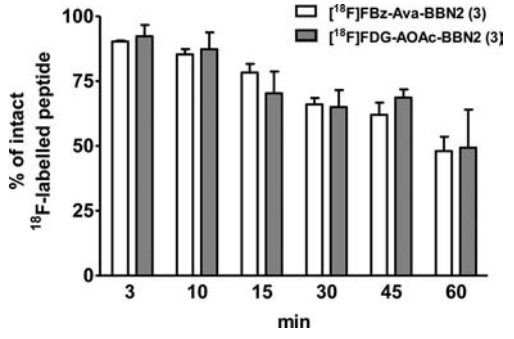

Figure 2. In vivo metabolic stability of [^{18}F]**FBz-Ava-BBN2** and [^{18}F]**FDG-AOAc-BBN2** over time. Data are shown as the percent of intact ^{18}F-labeled peptide and as mean ± SEM from n = 3 experiments.

DOI: 10.1021/bc500599m
Bioconjugate Chem. 2015, 26, 201−212

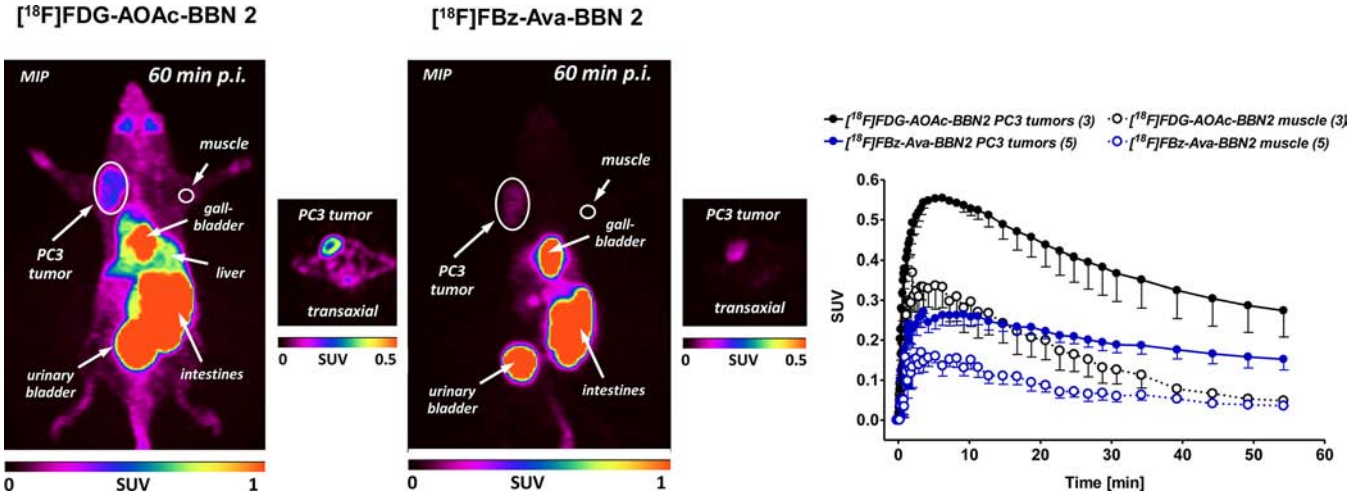

Figure 3. Representative PET images (MIP − maximum intensity projection and one transaxial slide) of a PC3 tumor-bearing BALB/c nude mouse 60 min after injection of [^{18}F]**FDG-AOAc-BBN2** or [^{18}F]**FBz-Ava-BBN2**. Images were generated on two subsequent days from the same mouse. The diagram on the right side shows the corresponding time−activity curves (TACs) for both radiotracers in PC3 tumors and muscle tissue. Data as mean ± SEM from *n* experiments.

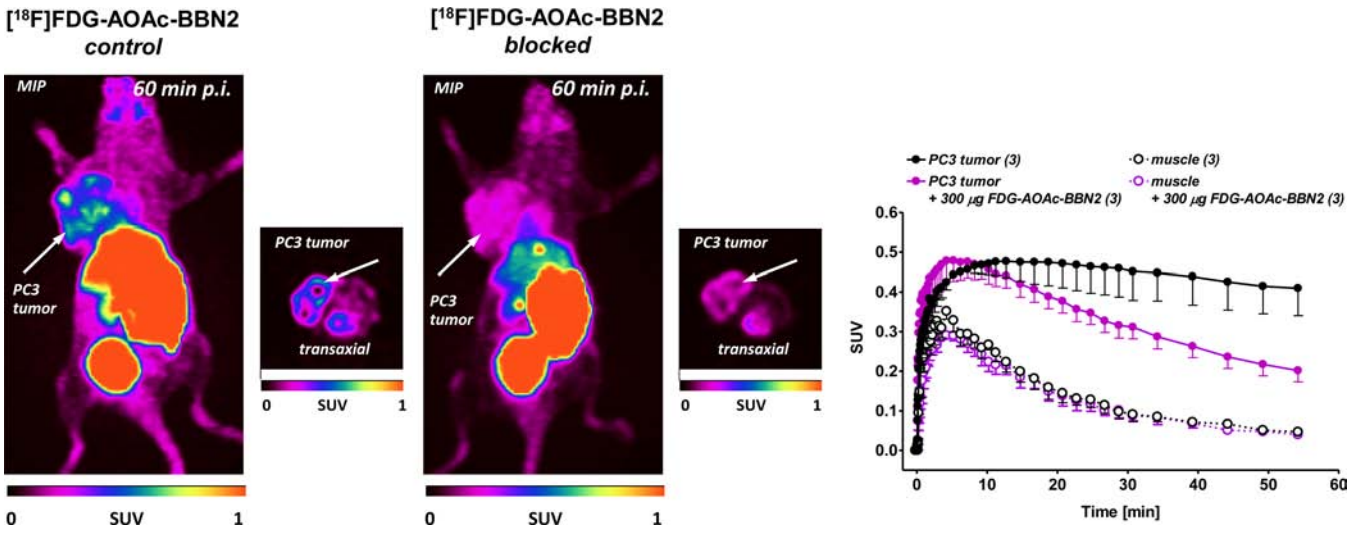

Figure 4. Representative PET images (MIP − maximum intensity projection and one transaxial slide) of a PC3 tumor-bearing BALB/c mouse in the absence (control) and presence of 300 μg nonlabeled FDG-AOAc-BBN2 after injection of [^{18}F]**FDG-AOAc-BBN2**. Images were generated on two subsequent days from the same mouse. The diagram on the right side shows the corresponding time−activity curves (TACs) in the absence and presence of the blocking agent in both PC3 tumors and muscle tissue. Data as mean ± SEM from *n* experiments.

min, both peptides showed some degradation, but their overall metabolic profile was comparable. After 60 min p.i., both peptides were found to be around 50% intact in the analyzed plasma samples. All detected radio-metabolites were more hydrophilic, and were not characterized further. Based on the radio-metabolite analysis it can be concluded that the oxime bond of [^{18}F]**FDG-AOAc-BBN2** is stable in vivo since only minute amounts of released [^{18}F]FDG could be detected in the plasma samples.

The GRP-receptor targeting properties of [^{18}F]**FDG-AOAc-BBN2** and [^{18}F]**FBz-Ava-BBN2** were studied in PC3 tumor-bearing BALB/c nude mice. Figure 3 depicts representative PET images at 60 min p.i. after injection of 2−5 MBq of [^{18}F]**FDG-AOAc-BBN2** (left) and [^{18}F]**FBz-Ava-BBN2** (right). Accumulation of radioactivity in the tumor is clearly visible in both images.

Figure 3 (right) also shows generated time−activity curves (TACs) for tumor and muscle uptake after injection of both radiolabeled peptides over 60 min. Maximum tumor accumulation levels were found after 5 min p.i. with standardized uptake values (SUV) of 0.55 ± 0.01 (n = 3) for [^{18}F]**FDG-AOAc-BBN2** and 0.26 ± 0.03 (n = 5) for [^{18}F]**FBz-Ava-BBN2.** Tumor accumulation slowly decreased over time resulting in $SUV_{60\ min}$ of 0.27 ± 0.07 (n = 3) for [^{18}F]**FDG-AOAc-BBN2** and 0.15 ± 0.03 (n = 5) for [^{18}F]**FBz-Ava-BBN2**, respectively.

Tumor accumulation and clearance pattern suggest a binding mode of both peptides as at least partially antagonistic. Both peptides showed rapid GRP-receptor-mediated accumulation in tumor tissue followed by low washout of radioactivity. The observed in vivo dissociation of radioactivity from tumor cells suggests that both radiolabeled peptides are not internalized. Recent analysis of FBz-Ava-BBN2 in an intracellular Ca^{2+}-releasing assay supports that conclusion.[32] The suggested predominant antagonistic binding mode is associated with better tumor targeting via more available binding sites

DOI: 10.1021/bc500599m
Bioconjugate Chem. 2015, 26, 201−212

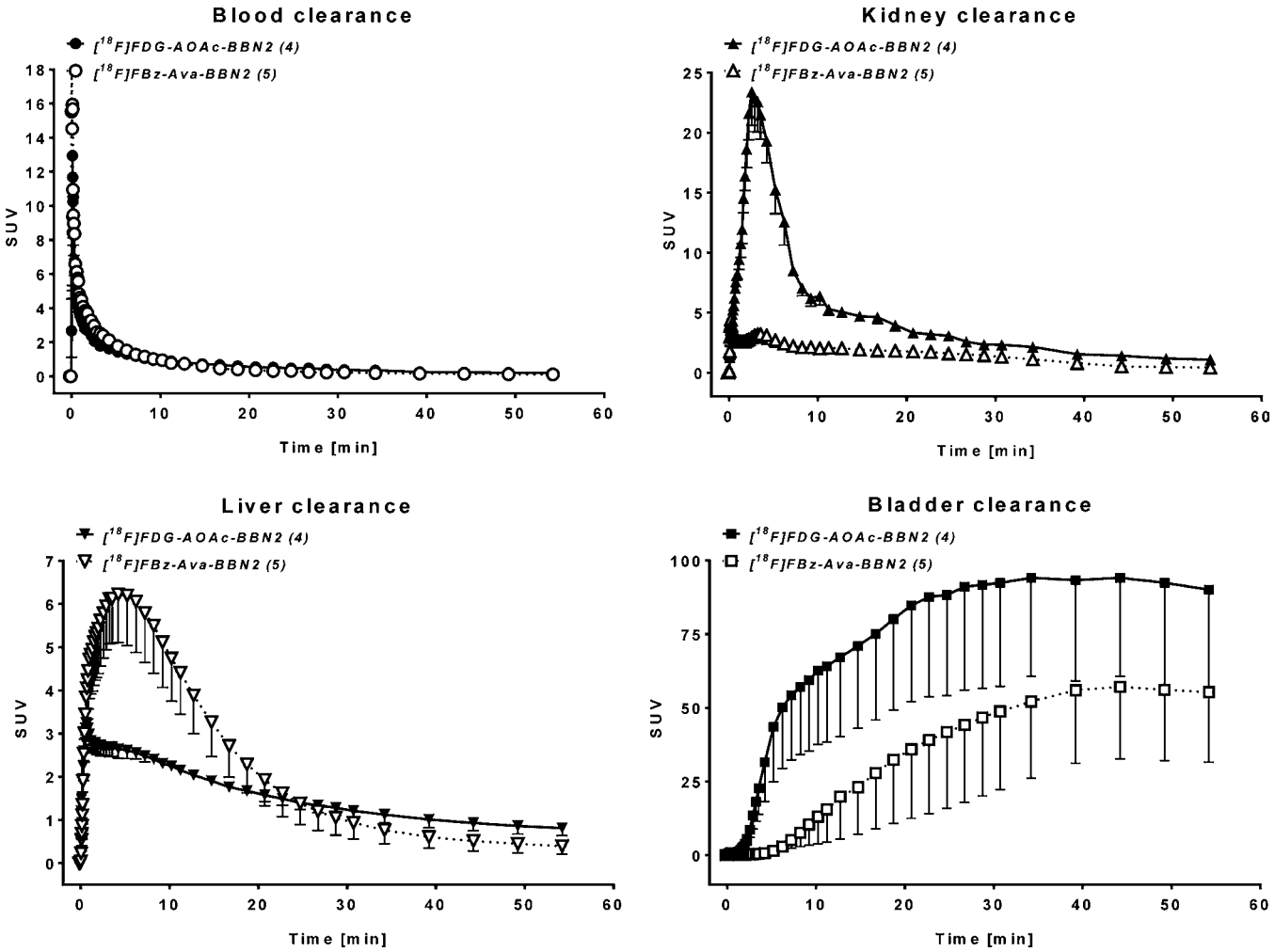

Figure 5. Time−activity curves (TACs) for clearance from blood (heart = blood pool), kidneys, and liver as well as detected radioactivity in the urinary bladder after injection of [^{18}F]**FDG-AOAc-BBN2** or [^{18}F]**FBz-Ava-BBN2** into PC3 tumor-bearing BALB/c nude mice. Data are presented as mean ± SEM from *n* experiments.

compared to the binding interaction with agonists. This is especially important for radiotherapy applications with radiolabeled peptides, and this finding was described by Cescato et al. as a change of paradigm.[36,37] The absence of internalization and the lack of induction of second messenger responses observed with antagonists offers another benefit when utilized for peptide receptor radiotherapy resulting in fewer pharmacological side effects. GRP receptor antagonism and GRP receptor specific uptake was recently determined for **FBz-Ava-BBN2** through blocking experiments.[32] Similar blocking studies in vivo were also performed with [^{18}F]**FDG-AOAc-BBN2** to confirm GRP receptor-mediated radiotracer uptake.

Figure 4 summarizes PET images representing the in vivo distribution of [^{18}F]**FDG-AOAc-BBN2** in the same PC3-bearing BALB/c nude mouse after 60 min p.i. as the control (left image) and after predosing with 300 μg nonradioactive **FDG-AOAc-BBN2** (right image). The blocking effect in tumor tissue was clearly visible.

The TACs determined clearly illustrate that PC3 tumor uptake of [^{18}F]**FDG-AOAc-BBN2** could significantly be blocked while the uptake and clearance pattern from muscle tissue was not affected (Figure 4 right). The $SUV_{60\ min}$ value of the tumor changed from 0.41 ± 0.07 to 0.20 ± 0.03, which represents a significant blocking effect of 50% (n = 3; p = 0.049). Consequently, tumor-to-muscle ratio was reduced from 8.2 ± 1.4 to 5.0 ± 0.7 (n = 3).

Thus, it can be concluded that the novel glycosylated bombesin analogue [^{18}F]**FDG-AOAc-BBN2** is interacting with the GRP receptor in vivo. Overall, tumor uptake of the more hydrophilic [^{18}F]FDG-labeled bombesin derivative [^{18}F]**FDG-AOAc-BBN2** was found to be about 2-fold higher compared to that of the more lipophilic [^{18}F]SFB-labeled compound [^{18}F]**FBz-Ava-BBN2**. This confirms the results of previous studies in which glycosylated peptides displayed higher tumor uptake.[24] Muscle uptake was also found to be different during the perfusion phase (0 to 10 min), while muscle uptake was comparable for both peptides at later time points (60 min p.i.) representing the metabolic phase ($SUV_{60\ min} \sim 0.5$). The switch of prosthetic groups from [^{18}F]SFB to [^{18}F]FDG resulted in only marginal changes in binding potencies (see IC_{50} values), but PC3 tumor uptake levels were significantly increased in the case of [^{18}F]FDG-labeled peptide [^{18}F]**FDG-AOAc-BBN2**. Since binding affinity toward the GRP receptor of both peptides is comparable, other factors must be responsible for the higher tumor uptake levels of [^{18}F]**FDG-AOAc-BBN2**, including pharmacokinetic parameters. One possible factor could be enhanced tissue penetration of [^{18}F]**FDG-AOAc-**

DOI: 10.1021/bc500599m
Bioconjugate Chem. 2015, 26, 201−212

Table 2. Biodistribution of [^{18}F]FDG-AOAc-BBN2 and [^{18}F]FBz-Ava-BBN2 in PC3 Tumor-Bearing BALB/c Nude Mice at 5 and 60 min Postinjection[a]

	[^{18}F]FDG-AOAc-BBN2		[^{18}F]FBz-Ava-BBN2	
organ	5 min p.i.	60 min p.i.	5 min p.i.	60 min p.i.
blood	11.24 ± 1.48	1.28 ± 0.49	15.20 ± 2.38	0.70 ± 0.14
heart	5.70 ± 0.99	2.04 ± 0.33	5.40 ± 1.32	0.28 ± 0.06
lung	8.38 ± 1.60	1.01 ± 0.30	5.90 ± 1.87	0.47 ± 0.05
liver	19.16 ± 2.50	9.09 ± 2.84	52.18 ± 4.96	4.07 ± 0.33
kidneys	55.24 ± 12.5	8.34 ± 1.79	12.10 ± 0.47	3.48 ± 0.61
spleen	2.57 ± 0.46	0.61 ± 0.16	2.83 ± 0.43	0.44 ± 0.11
stomach	2.34 ± 0.32	1.16 ± 0.46	1.86 ± 0.30	0.65 ± 0.09
duodenum	20.04 ± 6.51	14.86 ± 3.39	90.82 ± 29.8	24.87 ± 7.04
small intestine	6.94 ± 1.18	40.04 ± 13.7	14.44 ± 5.76	103.67 ± 23.0
large intestine	2.11 ± 0.55	13.12 ± 8.49	1.22 ± 0.07	3.60 ± 2.72
pancreas	4.94 ± 2.72	1.00 ± 0.29	5.44 ± 0.49	1.53 ± 0.22
bone	1.40 ± 0.45	0.21 ± 0.03	0.83 ± 0.09	0.17 ± 0.01
muscle	1.32 ± 0.50	0.50 ± 0.18	0.55 ± 0.10	0.16 ± 0.01
adrenals	3.55 ± 0.92	1.01 ± 0.26	3.06 ± 0.70	0.56 ± 0.14
brain	0.90 ± 0.18	0.22 ± 0.04	0.59 ± 0.06	0.04 ± 0.01
fat	1.47 ± 0.13	1.21 ± 0.69	1.76 ± 0.59	0.30 ± 0.09
PC3 tumor	4.11 ± 1.10	3.07 ± 0.61	1.17 ± 0.28	1.68 ± 0.19
tumor-to-blood ratio	0.35 ± 0.06	2.89 ± 0.90	0.09 ± 0.04	10.82 ± 1.70
tumor-to-muscle ratio	3.50 ± 0.81	9.53 ± 5.00	2.44 ± 1.00	2.52 ± 0.33

[a]Data are shown as percent of injected dose per gram of tissue (% ID/g) and as mean ± SEM and from n = 3 animals per time point.

BBN2. Increased tissue penetration properties were already demonstrated for various glycosylated peptides.[24]

In order to elucidate how prosthetic groups [^{18}F]SFB and [^{18}F]FDG influence metabolic pathways of both radiolabeled peptides, clearance patterns of selected tissues and organs were analyzed separately. Figure 5 depicts generated time−activity curves for regions of interest (ROIs) over the heart (representing the blood pool), liver, kidneys, and bladder.

As typical for small radiolabeled peptides, **[^{18}F]FDG-AOAc-BBN2** and **[^{18}F]FBz-Ava-BBN2** are both characterized by a fast blood clearance during the perfusion phase of the radiotracers, which is one reason for increasing tumor-to-blood ratios over time. No significant differences in blood clearance were observed for both radiolabeled peptides, despite that lipophilicity was changed significantly. On the other hand, elimination through the liver was affected by the selected prosthetic group. In comparison to **[^{18}F]FDG-AOAc-BBN2**, significantly higher liver uptake levels were found during the perfusion phase after the injection of more lipophilic peptide **[^{18}F]FBz-Ava-BBN2**. Liver clearance of less lipophilic peptide **[^{18}F]FDG-AOAc-BBN2** was slower resulting in slightly higher remaining liver activity after 60 min p.i. compared to **[^{18}F]FBz-Ava-BBN2**. However, resulting tumor-to-liver ratios (∼0.3 to 0.4) were not impaired.

Based on its higher lipophilicity, **[^{18}F]FBz-Ava-BBN2** was mainly excreted via the hepatobiliary pathway. In contrast, ^{18}F-glycosylated bombesin derivative **[^{18}F]FDG-AOAc-BBN2** was preferentially cleared through the kidneys resulting in about 5 times higher radioactivity levels during the perfusion phase compared to **[^{18}F]FBz-Ava-BBN2**. Higher activity levels in kidneys were found over the entire time course of the PET study in the case of **[^{18}F]FDG-AOAc-BBN2**. Radioactivity collected in the urinary bladder was also higher after injection of **[^{18}F]FDG-AOAc-BBN2** compared to **[^{18}F]FBz-Ava-BBN2**.

In the case of **[^{18}F]FBz-Ava-BBN2**, almost no or only a little radioactivity was detected in the bladder during the first 5 to 7 min, respectively. The more hydrophilic nature as reflected by the negative log D value of **[^{18}F]FDG-AOAc-BBN2** led to a predominantly renal elimination pathway. However, after 60 min p.i. there were also substantial amounts of radioactivity present in the intestines based on the portion of liver clearance.

In addition to the PET experiments, biodistribution studies were carried out with both peptides to further analyze radioactivity accumulation in PC3 tumors, organs, and tissues. Table 2 summarizes the biodistribution results of **[^{18}F]FDG-AOAc-BBN2** in comparison to **[^{18}F]FBz-Ava-BBN2** after 5 min (perfusion phase) and 60 min p.i. (metabolic phase) including tumor-to-blood and tumor-to-muscle ratios.

Both radiolabeled peptides showed fast and comparable clearance pattern from the blood and heart, which confirms TAC data derived from the PET imaging experiments. Radioactivity uptake was detected in GRP receptor-rich pancreas tissue with 4.94 ± 2.72%ID/g vs 5.44 ± 0.49%ID/g after 5 min p.i. **for** **[^{18}F]FDG-AOAc-BBN2** and **[^{18}F]FBz-Ava-BBN2**, respectively. Over time, radioactivity uptake in the pancreas decreased for both peptides.

The slightly higher radioactivity uptake found in the pancreas in the case of more lipophilic peptide **[^{18}F]FBz-Ava-BBN2** is in agreement with recent observations reported by Varasteh et al.[38] PC3 tumor uptake was found to be 4.11 ± 1.10%ID/g for **[^{18}F]FDG-AOAc-BBN2** at 5 min p.i., which decreased over time reaching 3.07 ± 0.61%ID/g at 60 min p.i. An almost 2-fold lower initial tumor uptake of 1.68 ± 0.19%ID/g was observed with **[^{18}F]FBz-Ava-BBN2** at 60 min p.i. The found PC3 tumor uptake pattern confirmed the data obtained from the dynamic PET imaging studies (Figure 3). The differences in tumor uptake of both peptides cannot be explained by differences in their inhibitory potency toward the GRP receptor or blood residence time differences as they are almost identical for both peptides. On the other hand, both peptides showed significant differences in their lipophilicity, ranging from a negative $\log D_{7.4}$ value of −0.73 for glycosylated peptide **[^{18}F]FDG-AOAc-BBN2** to a positive $\log D_{7.4}$ value of +1.22 for fluorobenzoylated peptide **[^{18}F]FBz-Ava-BBN2**. A recent study with various

DOI: 10.1021/bc500599m
Bioconjugate Chem. 2015, 26, 201−212

glycosylated RGD peptides possessing different lipophilicities demonstrated that despite the differences in lipophilicity the blood clearance was comparable for all studied peptides. The authors concluded that lipophilicity of their peptides seems not to be a critical parameter for blood clearance.[39] Thus, other factors like plasma protein binding kinetics and tissue penetrating properties are likely to contribute to the observed differences in tumor uptake as confirmed through our biodistribution and PET imaging experiments. However, the exact mechanisms behind the observed differences in the tumor uptake of peptides [^{18}F]**FDG-AOAc-BBN2** and [^{18}F]**FBz-Ava-BBN2** remain unclear.

Data in Table 2 show that the tumor-to-muscle ratio of [^{18}F]**FDG-AOAc-BBN2** was higher compared to that of [^{18}F]**FBz-Ava-BBN2**, being 9.53 ± 5.00 vs 2.52 ± 0.33 after 60 min p.i. Both peptides showed almost no brain uptake, and the initial brain uptake of radioactivity was washed out over time, reaching brain activity of 0.22 ± 0.04%ID/g for [^{18}F]**FDG-AOAc-BBN2** and 0.04 ± 0.01%ID/g for [^{18}F]**FBz-Ava-BBN2** after 60 min p.i. This is indicative that both peptides are not capable of crossing the blood-brain-barrier. The absence of significant radioactivity accumulation in the bone over time precludes radiodefluorination of both peptides and confirms the stability of the radiolabel ^{18}F in both peptides.

The biodistribution pattern of both peptides in major elimination and metabolism organs like kidneys and liver was in alignment with the observed changes in elimination pathways obtained from dynamic PET imaging experiments. This further confirms the proposed rerouting concept of the metabolic pathway by the selection of the ^{18}F-labeled prosthetic group. [^{18}F]**FDG-AOAc-BBN2** showed high initial radioactivity accumulation in the kidneys (55.24 ± 12.5%ID/g) after 5 min p.i. while the uptake of peptide [^{18}F]**FBz-Ava-BBN2** was much lower at 5 min p.i. (12.10 ± 0.47%ID/g). This finding also agrees with data obtained from dynamic PET imaging experiments, and it can be concluded that less lipophilic peptide [^{18}F]**FDG-AOAc-BBN2** is predominantly cleared through the renal elimination system. On the other hand, the initial liver uptake of peptide [^{18}F]**FDG-AOAc-BBN2** was significantly lower at 5 min p.i. (19.16 ± 2.50%ID/g) compared to the high initial liver uptake at 5 min p.i. of more lipophilic peptide [^{18}F]**FBz-Ava-BBN2** (52.18 ± 4.96%ID/g). Additional differences in the elimination pathways of both peptides were further clearly visible in the high radioactivity accumulation of 103.67 ± 23.0%ID/g at 60 min p.i. in small intestines for peptide [^{18}F]**FBz-Ava-BBN2**, whereas peptide [^{18}F]**FDG-AOAc-BBN2** showed much lower radioactivity accumulation in small intestines of 40.04 ± 13.7%ID/g at 60 min p.i.. The biodistribution pattern found confirm the preferred hepatobiliary elimination pathway of more lipophilic peptide [^{18}F]**FBz-Ava-BBN2** in comparison to the predominant renal elimination pathway of less lipophilic peptide [^{18}F]**FDG-AOAc-BBN2**.

Thus, data from both biodistribution and dynamic PET imaging experiments confirm significant differences of the elimination pathway of radiolabeled peptides [^{18}F]**FBz-Ava-BBN2** and [^{18}F]**FDG-AOAc-BBN2** influenced by the selected prosthetic group. A switch from [^{18}F]SFB to [^{18}F]FDG as the prosthetic group for peptide labeling acts as a pharmacokinetic modifier. The predominant hepatobiliary clearance of more lipophilic [^{18}F]SFB-labeled bombesin derivative [^{18}F]**FBz-Ava-BBN2** is rerouted toward a more preferred renal elimination pathway in the case of more hydrophilic [^{18}F]FDG-labeled bombesin derivative [^{18}F]**FDG-AOAc-BBN2**. Among other but still unknown factors, these differences in the clearance pattern of peptides [^{18}F]**FBz-Ava-BBN2** and [^{18}F]**FDG-AOAc-BBN2** may also contribute to the observed differences of radioactivity uptake in GRP receptor expressing PC3 tumors.

Interestingly, the incorporation of chemically quite different prosthetic groups [^{18}F]SFB (a fluorobenzoic acid active ester) and [^{18}F]FDG (a fluorinated glucose) into GRP receptor targeting the peptide backbone QWAV-Sar-H-FA01010-Tle-NH_2 resulted in radiolabeled peptides with comparable blood clearance pattern, comparable inhibitory potencies, and similar metabolic stabilities. Based on these observations and findings it can be concluded that glycosylated peptide [^{18}F]**FDG-AOAc-BBN2** represents a more suitable PET radiotracer for molecular imaging of GRP receptors compared to previously reported [^{18}F]**FBz-Ava-BBN2**.

■ CONCLUSION

In summary, the present study demonstrates that the use of prosthetic groups [^{18}F]SFB and [^{18}F]FDG results in a modification of pharmacokinetics of ^{18}F-labeled bombesin derivatives. Accordingly, rerouting of elimination pathways can conveniently be achieved through selection of the prosthetic group for peptide labeling with ^{18}F. Based on its higher uptake levels in GRP receptor-expressing prostate cancer cells, novel ^{18}F-labeled carbohydrated and stabilized bombesin derivative [^{18}F]**FDG-AOAc-BBN2** represents a superior PET radiotracer for molecular imaging of GRP-receptors compared with [^{18}F]**FBz-Ava-BBN2**. The beneficial metabolic stability, along with higher tumor accumulation levels as well as more favorable renal excretion, supports the use of [^{18}F]**FDG-AOAc-BBN2** for PET imaging of GRP receptors in prostate cancer. However, further structural fine-tuning of radiopeptides like [^{18}F]**FDG-AOAc-BBN2** is necessary to allow for optimal GRP receptor imaging in prostate cancer patients. This would include improvement of inhibitory potency to reduce dissociation from GRP receptors on the tumor, faster renal elimination, and faster muscle clearance to enhance image quality also at earlier time points. The concept of rerouting utilizing [^{18}F]FDG as a prosthetic group to introduce the radiolabel and while modifying metabolism can also be extended to other peptides targeting different receptors and/or enzymes in order to optimize radiopharmacokinetics along with enhanced tumor accumulation levels.

■ EXPERIMENTAL SECTION

General. All peptide synthesis reagents were purchased from NovaBioChem except modified Fmoc-amino acid FA01010 ((4*R*,5*S*)-Fmoc-4-amino-5-methylheptanoic acid) and the linker Fmoc-Ava-OH, which were obtained from Polypeptide Inc. (USA). Stabilized bombesin peptide amides were synthesized in a combination of manual coupling procedures and automated solid phase peptide synthesis (SPPS) using the Syro I peptide synthesizer (MultiSynTech/Biotage, USA). Mass spectra were recorded on an Agilent 620oaTOF electron spray ionization mass spectrometer (ESI-MS). Analytical HPLC was performed on a Shimadzu system equipped with a DGU-20A5 degasser, an SIL-20A HT autosampler, a LC-20AT pump, a SPD-M20A photodiode-array detector, and a Ramona Raytest radiodetector using a Phenomenex Luna 10u C18(2) 100A, 250 × 4.6 mm column.

DOI: 10.1021/bc500599m
Bioconjugate Chem. 2015, 26, 201−212

Semipreparative HPLC was performed on a Gilson system with a 321 pump, a photodiode array detector, and a HERM Bertolt radiodetector installed with a Phenomenex Jupiter 10u Proteo 90A, 250 × 10 mm, 4.5 μm C18 column. UV absorbance was monitored at 210 nm wavelength. The mobile phase consisted of water/0.2%TFA as solvent A and acetonitrile as solvent B.

N-Succinimidyl-4-[^{18}F]fluorobenzoate ([^{18}F]SFB) and 2-deoxy-2-[^{18}F]fluoro-D-glucose ([^{18}F]FDG) were used as peptide radiolabeling agents in a prosthetic group approach. The synthesis of [^{18}F]SFB was performed in the two-pot three-step reaction reported by Maeding et al.[40] using a TRACERlab FX automated synthesis unit from GE Healthcare providing the prosthetic group in radiochemical yields of 71 ± 20% (decay-corrected) and radiochemical purities of greater than 95% in less than 60 min synthesis time. [^{18}F]FDG was used from the routine clinical batches as produced at the Edmonton PET Centre according to Hamacher et al.[41] established on a TRACERlab MX automated synthesis unit (GE Healthcare).

For in vitro binding studies human androgen-independent prostate cancer cell line PC3 (American Type Tissue Culture Centre, USA) was cultivated in 45% RPMI1640 Dulbecco's modified Eagle's medium (DMEM) supplemented with 45% Ham's F-12 and 10% heat-inactivated fetal bovine serum (FBS) from Invitrogen (USA). ^{125}I-Tyr^4-BBN was from PerkinElmer (USA). Cell-associated radioactivity was measured on a 2480 Automatic gamma counter WIZARD^2 (PerkinElmer, USA).

All animal studies were carried out according to the guidelines of the Canadian Council on Animal Care (CCAC) and approved by the Cross Cancer Institute Animal-Care Committee. In vivo studies were done using normal BALB/c and male PC3-tumor-bearing BALB/c Nude mice (body weight: ∼21.0 g). For tumor xenografts, about (3−4) × 10^6 PC3 cells in 100 μL culture medium were injected subcutaneously. After 4−5 weeks, tumors reached sizes of ∼300−400 mm^3 and were used for the experiments described. PET studies were performed on an INVEON PET/CT scanner (SiemensPreclinical Solutions, Knoxville, USA).

Peptide Synthesis. Stabilized bombesin peptides were synthesized using the Fmoc-orthogonal solid phase peptide synthesis starting from the Rink Amide MBHA resin (loading: 0.6 mmol/g). Detailed description on the synthetic procedure and cleavage conditions of the bombesin sequence Ava-Gln^7-Trp^8-Ala^9-Val^{10}-Sar^{11}-His^{12}-FA01010^{13}-Tle^{14}-NH$_2$ (**Ava-BBN2**) and corresponding reference peptide FBz-Ava-Gln^7-Trp^8-Ala^9-Val^{10}-Sar^{11}-His^{12}-FA01010^{13}-Tle^{14}-NH$_2$ (**FBz-Ava-BBN2**) can be found in a previously published manuscript.[32]

Ava-Gln^7-Trp^8-Ala^9-Val^{10}-Sar^{11}-His^{12}-FA01010^{13}-Tle^{14}-NH$_2$ ***Ava-BBN2***. Peptide **Ava-BBN2** was elongated on 100 mg solid support Rinkamide MBHA resin using 5 equiv each of Fmoc-amino acid building block coupled with HBTU/Oxyma/DIPEA 1:1:2. Total cleavage, purification via semipreparative HPLC (2 mL/min, 0−5 min 30% B, 35 min 55% B, 40−50 min 70% B; t_R = 11.8 min) and lyophilization delivered **Ava-BBN2** as white powder (17.0 mg (16 μmol), 27% yield, >97% purity). MW $C_{52}H_{82}N_{14}O_{10}$ 1062.6, found LR-ESI-MS (positive) m/z 1063.6 [M + H]$^+$, 1085.6 [M + Na]$^+$, 532.3 [M+2H]$^{2+}$.

FBz-Ava-Gln^7-Trp^8-Ala^9-Val^{10}-Sar^{11}-His^{12}-FA01010^{13}-Tle^{14}-NH$_2$ ***FBz-Ava-BBN2***. Starting from 12.5 mg Rinkamide MBHA resin following total cleavage, purification via semipreparative HPLC (2 mL/min, 0−30 min from 10% B to 60% B, 35 min 60% B; t_R = 30.1 min) and lyophilization reference peptide **FBz-Ava-BBN2** gave a white powder (1.5 mg (1.3 μmol), 17% yield, >95% purity). MW $C_{59}H_{85}FN_{14}O_{11}$ 1184.7, found LR-ESI-MS (positive) m/z 1185.7 [M + H]$^+$.

Synthesis of Aminooxy-acetyl-Gln^7-Trp^8-Ala^9-Val^{10}-Sar^{11}-His^{12}-FA01010^{13}-Tle^{14}-NH$_2$ ***AOAc-BBN2***. 50 mg Rink Amide MBHA resin was used to synthesize 8-amino-acid peptide **AOAc-BBN2**. Aminooxy acetic acid was incorporated as terminal building block using the Boc-protected derivative Boc-aminooxy acetic acid. The desired peptide amide was isolated after total cleavage, semipreparative HPLC purification (2 mL/min, 0−5 min 30% B, 35 min 60% B, 40 min 70% B; t_R = 12.3 min) and subsequent lyophilization as a powder (10.9 mg (10.5 μmol), 30% yield, >99% purity). MW $C_{49}H_{76}N_{14}O_{11}$ 1036.6, found LR-ESI-MS (positive) m/z 1037.6 [M + H]$^+$, 519.3 [M+2H]$^{2+}$.

Preparation of 2-([(E)-(2-Fluoro-3,4,5,6-tetrahydroxyhexylidene)amino]oxy)acetyl-Gln^7-Trp^8-Ala^9-Val^{10}-Sar^{11}-His^{12}-FA01010^{13}-Tle^{14}-NH$_2$ ***FDG-AOAc-BBN2***. A solution of 2.1 mg (2.0 μmol, 1 equiv) **AOAc-BBN2** in 50 μL methanol and 0.6 mg (3.3 μmol, 1.6 equiv) 2-fluoro-2-deoxy-D-glucose (FDG) in 50 μL water were mixed and incubated for 2 h at 85 °C. The reaction mixture was injected onto a HPLC for purification (2 mL/min, 0−5 min 20% B, 10 min 35% B, 25 min 50% B, 30−35 min 70% B; t_R = 22.2 min) revealing over 95% **FDG-AOAc-BBN2** (isomers result in a characteristic double peak). HPLC solvent was reduced under vacuum using a rotary evaporator and subsequently lyophilized to give a white powder (1.5 mg (1.3 μmol), 63% yield, >95% purity). MW $C_{55}H_{85}FN_{14}O_{15}$ 1200.6, found LR-ESI-MS (positive) m/z 1201.6 [M + H]$^+$, 601.3 [M+2H]$^{2+}$.

Competitive Binding Assay. In vitro competitive binding was analyzed in human prostate adenocarcinoma PC3 cells in triplicate as described before.[32] Briefly, determination of the concentration of half-maximum inhibition (IC_{50} values) was carried out as a competition against ^{125}I-Tyr^4-bombesin (0.05 nM final concentration) using increasing concentrations of **FBz-Ava-BBN2** or **FDG-AOAc-BBN2** in the range of 5 pM to 0.5 μM. After incubation for 2 h at 4 °C and several washing steps, the cells were harvested. Counts per minute (cpm) of cell-associated radioactivity were measured in a Wizard gamma counter, decay corrected, and plotted versus log of the peptide concentration to give the typical sigmoidal dose−response curves.

Radiolabeling of Bombesin Derivatives with Prosthetic Groups [^{18}F]SFB and [^{18}F]FDG. *Radiolabeling of Bombesin Peptide* ***Ava-BBN2*** *with [^{18}F]SFB ([^{18}F]FBz-Ava-BBN2) (n = 15).* *N*-Terminal ^{18}F-fluorobenzoylation of **Ava-BBN2** was achieved by employing 0.5 mg peptide in 200 μL 50 mM Na_2HPO_4 buffer (pH 9) and subsequent incubation with 100 μL [^{18}F]SFB/MeCN at 40 °C for 30 min. Semipreparative radio-HPLC purification (2 mL/min, 0−5 min 20% B, 10 min 35% B, 25 min 50% B, 30−35 min 70% B; t_R = 24.3 min) and removing the HPLC solvent under vacuum yielded the desired peptide. 100−150 μL 0.9% saline was used to prepare the product as injectable solution. Overall synthesis time: 86 ± 2 min. RCY: 52 ± 8%. RCP: 95.0−99.8%. $A_S \gg 40$ GBq/μmol. Quality control of the product was performed on an analytical HPLC system (1 mL/min, 0−3 min 10% B, 7 min 25% B, 13 min 35% B, 17 min 50% B, 23 min 70% B, 27−30 min 90% B; t_R = 19.8 min).

Radiolabeling of Bombesin Peptide ***AOAc-BBN2*** *with [^{18}F]FDG ([^{18}F]FDG-AOAc-BBN2) (n = 10).* [^{18}F]FDG was used as supplied by the Edmonton PET Centre without further purification from D-glucose. A modified procedure to the

DOI: 10.1021/bc500599m
Bioconjugate Chem. 2015, 26, 201−212

published methods for ^{18}F-FDG oximation of peptides[28,33,34] was applied for the labeling of aminooxy-functionalized bombesin derivative **AOAc-BBN2**. In a LoBind Eppendorf tube, 50−100 μL [^{18}F]FDG/saline were added to 0.5 mg **AOAc-BBN2** dissolved in 70 μL methanol. The reaction mixture was allowed to incubate at 85 °C for 45 min after the addition of 1 μL aniline. Semipreparative purification was performed on radio-HPLC (2 mL/min, 0−5 min 20% B, 10 min 35% B, 25 min 50% B, 30−35 min 70% B; t_R = 21.0 min) and the fractions containing the ^{18}F-glycosylated peptide were collected and subjected to a rotary evaporator to remove the MeCN/water/0.2%TFA HPLC solvent. Product was redissolved in 100−150 μL 0.9% saline for delivery of the injectable formulation. Overall synthesis time: 88 ± 2 min. RCY: 51 ± 24%. RCP: 95.0−99.8%. A_S ≫ 40 GBq/μmol. Quality control of the product was performed on an analytical HPLC system (1 mL/min, 0−3 min 10% B, 7 min 25% B, 13 min 35% B, 17 min 50% B, 23 min 70% B, 27−30 min 90% B; t_R = 17.1 min).

Determination of Radiopeptide Lipophilicity. Lipophilicity was obtained according to the shake-flask method[42] by determining the partition coefficient of the ^{18}F-labeled peptide in *n*-octanol and PBS buffer (pH 7.4) as aqueous phase. The organic and the aqueous phase were presaturated 24 h before the actual start of the experiment. 500 μL aliquots of each layer were added to 300−2000 kBq of [^{18}F]**FBz-Ava-BBN2** or [^{18}F]**FDG-AOAc-BBN2** in a LoBind Eppendorf tube and the mixture was shaken intensely for 5 min. The layers were allowed to separate by centrifugation at 2000 rpm for 2 min. Aliquots of 100 μL were removed from each phase and measured in a gamma counter. Calculated $\log D_{7.4}$ values are expressed as mean ± SD and summary of 3 experiments each performed in triplicate.

In Vivo Metabolic Stability Studies. Normal BALB/c mice were injected with 10−20 MBq of [^{18}F]**FBz-Ava-BBN2** or [^{18}F]**FDG-AOAc-BBN2**, respectively. Venous blood samples were collected at 3, 10, 15, 30, 45, and 60 min postinjection via the mouse tail vein and further processed. Blood cells were separated by centrifugation (13 000 rpm × 5 min). Precipitation of proteins in the supernatant was achieved by addition of 2 volume parts of methanol, and samples were centrifuged again (13 000 rpm × 5 min). Fractions of blood cells, proteins, and plasma were measured in a Wizard gamma counter to determine radioactivity per sample. The clear plasma supernatant was injected onto a Shimadzu HPLC system. The samples were analyzed using a Phenomenex Luna 10u C18(2) 100A, 250 × 4.6 mm column at a constant flow rate of 1 mL/min and the following gradient with water/0.2% TFA as solvent A and acetonitrile as solvent B: 0−3 min 10% B, 10 min 30% B, 17 min 50% B, 23 min 70% B, 27−30 min 90% B.

Small Animal PET Studies. PET imaging of radiopeptides [^{18}F]**FBz-Ava-BBN2** and [^{18}F]**FDG-AOAc-BBN2** was performed using male PC3 tumor-bearing BALB/c nude mice to determine tumor uptake, distribution, and clearance parameters. Prior to the radiotracer injection, mice were anesthetized through inhalation of isoflurane in 40% oxygen/60% nitrogen (gas flow 1 L/min), and body temperature was kept constant at 37 °C. Mice were positioned in a prone position into the center of the field of view. A transmission scan for attenuation correction was not acquired. Mice were injected with 2−5 MBq [^{18}F]**FBz-Ava-BBN2** or [^{18}F]**FDG-AOAc-BBN2** (60−150 ng) in 150 μL isotonic sodium chloride solution (0.9%) through a tail vein catheter. For blocking studies, animals were predosed with 300 μg ^{19}FDG-AOAc-BBN2 in 50 μL saline about 10 min prior to radiotracer injection. Data acquisition was performed over 60 min in 3D list mode. The dynamic list mode data were sorted into sinograms with 53 time frames (10 × 2, 8 × 5, 6 × 10, 6 × 20, 8 × 60, 10 × 120, 5 × 300 s). The frames were reconstructed using maximum a posteriori (MAP) as reconstruction mode. The pixel size was 0.085 by 0.085 by 0.121 mm^3 (256 × 256 × 63) and the resolution in the center of the field of view was 1.8 mm. No correction for partial volume effects was applied. The image files were processed using the ROVER v 2.0.51 software (ABX GmbH, Radeberg, Germany). Masks defining 3D regions of interest (ROI) were set and the ROIs were defined by thresholding. Mean standardized uptake values [SUV_{mean} = (activity/mL tissue)/(injected activity/body weight), mL/g] were calculated for each ROI. Time-activity curves (TAC) were generated for the dynamic scans only. All semiquantified PET data are presented as means ± SEM. Statistical difference for the blocking study was tested by unpaired Student's *t*-test and was considered significant for $P < 0.05$.

Biodistribution Studies. Biodistribution studies were performed in male PC3 tumor-bearing BALB/c nude mice. After intravenous injection of 1−2 MBq [^{18}F]**FBz-Ava-BBN2** or [^{18}F]**FDG-AOAc-BBN2** in 150 μL saline (0.9% w/v of NaCl) into the tail vein of anesthetized mice, the animals were allowed to regain consciousness until sacrifice. Animals were euthanized by decaptation at 5 and 60 min post injection and rapidly dissected. Organs of interest including blood, heart, lung, liver, kidneys, spleen, duodenum, small and large intestine, pancreas, right femur, muscle, brain, fat, and tumor were collected and weighed. Radioactivity in all tissues was measured in the γ-counter, and results were analyzed as percentage of injected dose per gram of tissue (%ID/g). Experiments were performed in triplicate for each time point. Data is represented as mean ± SEM.

■ ASSOCIATED CONTENT

Ⓢ Supporting Information

HPLC system and chromatograms. This material is available free of charge via the Internet at http://pubs.acs.org.

■ AUTHOR INFORMATION

Corresponding Author

*E-mail: wuest@ualberta.ca.

Notes

The authors declare no competing financial interest.

■ ACKNOWLEDGMENTS

The authors would like to thank John Wilson, Dave Clendening, and Blake Lazurko from the Edmonton PET Centre for radionuclide production as well as Angela Westover and Jeff McPherson for providing [^{18}F]FDG. F.W. thanks the Dianne and Irving Kipnes Foundation for supporting this work.

■ REFERENCES

(1) Fani, M., Maecke, H. R., and Okarvi, S. M. (2012) Radiolabeled peptides: valuable tools for the detection and treatment of cancer. *Theranostics 2*, 481−501.

(2) Laverman, P., Sosabowski, J. K., Boerman, O. C., and Oyen, W. J. (2012) Radiolabelled peptides for oncological diagnosis. *Eur. J. Nucl. Med. Mol. Imaging 39* (Suppl1), S78−92.

(3) Lozza, C., Navarro-Teulon, I., Pèlegrin, A., Pouget, J. P., and Vivès, E. (2013) Peptides in receptor-mediated radiotherapy: from design to the clinical application in cancers. *Front. Oncol. 3*, 247.

DOI: 10.1021/bc500599m
Bioconjugate Chem. 2015, 26, 201−212

(4) Koopmans, K. P., and Glaudemans, A. W. (2012) Rationale for the use of radiolabelled peptides in diagnosis and therapy. *Eur. J. Nucl. Med. Mol. Imaging 39* (Suppl 1), S4−10.
(5) Graham, M. M., and Menda, Y. (2011) Radiopeptide imaging and therapy in the United States. *J. Nucl. Med. 52*, 56S−63S.
(6) Fani, M., and Maecke, H. R. (2012) Radiopharmaceutical development of radiolabelled peptides. *Eur. J. Nucl. Med. Mol. Imaging 39* (Suppl 1), S11−S30.
(7) Jensen, R. T., Battey, J. F., Spindel, E. R., and Benya, R. V. (2008) International Union of Pharmacology. LXVIII. Mammalian bombesin receptors: Nomenclature, distribution, pharmacology, signaling, and functions in normal and disease states. *Pharmacol. Rev. 60*, 1−42.
(8) Jensen, J. A. G., Carroll, R. E., and Benya, R. V. (2001) The case for gastrin-releasing peptide acting as a morphogen when it and its receptor are aberrantly expressed in cancer. *Peptides 22*, 689−99.
(9) Markwalder, R., and Reubi, J. C. (1999) Gastrin-releasing peptide receptors in the human prostate: relation to neoplastic transformation. *Cancer Res. 59*, 1152−59.
(10) Mansi, R., Fleischmann, A., Maecke, H. R., and Reubi, J. C. (2013) Targeting GRPR in urological cancers − from basic research to clinical application. *Nat. Rev. Urol. 10*, 235−44.
(11) Sancho, V., Di Florio, A., Moody, T. W., and Jensen, R. T. (2011) Bombesin receptor-mediated imaging and cytotoxicity: Review and current status. *Curr. Drug Delivery 8*, 79−134.
(12) Yu, Z., Ananias, H. J. K., Carlucci, G., Hoving, H. D., Helfrich, W., Dierckx, RAJO, Wang, F., de Jong, I. J., and Elsinga, P. H. (2013) An update of radiolabeled bombesin analogs for gastrin-releasing peptide receptor targeting. *Curr. Pharm. Des. 19*, 3329−41.
(13) Hohla, F., and Schally, A. V. (2010) Targeting gastrin releasing peptide receptors: New options for the therapy and diagnosis of cancer. *Cell Cycle 9*, 1738−41.
(14) Schroeder, R. P., van Weerden, W. M., Bangma, C., Krenning, E. P., and de Jong, M. (2009) Peptide receptor imaging of prostate cancer with radiolabelled bombesin analogues. *Methods 48*, 200−4.
(15) Cescato, R., Maina, T., Nock, B., Nikolopoulou, A., Charalambidis, D., Piccand, V., and Reubi, J. C. (2008) Bombesin receptor antagonists may be preferable to agonists for tumor targeting. *J. Nucl. Med. 49*, 318−26.
(16) Schroeder, R. P., Müller, C., Reneman, S., Melis, M. L., Breeman, W. A., de Blois, E., Bangma, C. H., Krenning, E. P., van Weerden, W. M., and de Jong, M. (2010) A standardised study to compare prostate cancer targeting efficacy of five radiolabelled bombesin analogues. *Eur. J. Nucl. Med. Mol. Imaging 37*, 1386−96.
(17) Yang, M., Gao, H., Zhou, Y., Ma, Y., Quan, Q., Lang, L., Chen, K., Niu, G., Yan, Y., and Chen, X. (2011) F-Labeled GRPR agonists and antagonists: a comparative study in prostate cancer imaging. *Theranostics 1*, 220−9.
(18) Wieser, G., Mansi, R., Grosu, A. L., Schultze-Seemann, W., Dumont-Walter, R. A., Meyer, P. T., Maecke, H. R., Reubi, J. C., and Weber, W. A. (2014) Positron emission tomography (PET) imaging of prostate cancer with a gastrin releasing peptide receptor antagonist - from mice to men. *Theranostics 4*, 412−9.
(19) Nanda, P. K., Wienhoff, B. E., Rold, T. L., Sieckman, G. L., Szczodroski, A. F., Hoffman, T. J., Rogers, B. E., and Smith, C. J. (2012) Positron-emission tomography (PET) imaging agents for diagnosis of human prostate cancer: agonist vs. antagonist ligands. *In vivo 26*, 583−92.
(20) Zhang, H., Abiraj, K., Thorek, D. L., Waser, B., Smith-Jones, P. M., Honer, M., Reubi, J. C., and Maecke, H. R. (2012) Evolution of bombesin conjugates for targeted PET imaging of tumors. *PLoS One 7*, e44046.
(21) Bubendorf, L., Schoepfer, A., Wagner, U., Sauter, G., Moch, H., Willi, N., Gasser, T. C., and Mihatsch, M. J. (2000) Metastatic patterns of prostate cancer: an autopsy study of 1,589 patients. *Human Pathology 31*, 578−83.
(22) Hosseinimehr, S. J., Tolmachev, V., and Orolova, A. (2012) Liver uptake of radiolabeled targeting proteins and peptides: considerations for targeting peptide conjugate design. *Drug Discovery Today 17*, 1224−1232.
(23) Lindner, S., Michler, C., Leidner, S., Michler, C., Waengler, C., Schirrmacher, R., Bartenstein, P., and Waengler, B. (2014) Synthesis and in vitro and in vivo evaluation of SiFA-tagged bombesin and RGD peptides as tumor imaging probes for positron emission tomography. *Bioconjugate Chem. 25*, 738−49.
(24) Wester, H. J., Schottelius, M., Poethko, T., Bruus-Jensen, K., and Schwaiger, M. (2004) Radiolabeled carbohydrated somatostatin analogs: a review of the current status. *Cancer Biother. Radiopharm. 19*, 231−44.
(25) Wieder, H., Beer, A. J., Poethko, T., Meisetschlaeger, G., Wester, H. J., Rummeny, E., Schwaiger, M., and Stahl, A. R. (2008) PET/CT with Gluc-Lys-([(18)F]FP)-TOCA: correlation between uptake, size and arterial perfusion in somatostatin receptor positive lesions. *Eur. J. Nucl. Med. Mol. Imaging 35*, 264−71.
(26) Haubner, R., Kuhnast, B., Mang, C., Weber, W. A., Kessler, H., Wester, H. J., and Schwaiger, M. (2004) [^{18}F]Galacto-RGD: synthesis, radiolabeling, metabolic stability, and radiation dose estimates. *Bioconjugate Chem. 15*, 61−9.
(27) Beer, A. J., and Schwaiger, M. (2011) PET imaging of $\alpha v\beta 3$ expression in cancer patients. *Methods Mol. Biol. 680*, 183−200.
(28) Wuest, F., Hultsch, C., Berndt, M., and Bergmann, R. (2009) Direct labeling of peptides with 2-[18F]fluoro-2-deoxy-d-glucose ([18F]FDG). *Bioorg. Med. Chem. Lett. 19*, 5426−28.
(29) Namavari, M., Cheng, Z., Zhang, R., De, A., Levi, J., Hoerner, J. K., Yaghoubi, S. S., Syud, F. A., and Gambhir, S. S. (2009) A novel method for direct site-specific radiolabeling of peptides using [18F]FDG. *Bioconjugate Chem. 20*, 432−6.
(30) Hoehne, A., Mu, L., Honer, M., Schubiger, P. A., Ametamey, S. M., Graham, K., et al. (2008) Synthesis, ^{18}F-labeling, and in vitro and in vivo studies of bombesin peptides modified with silicon-based building blocks. *Bioconjugate Chem. 19*, 1871−9.
(31) Mu, L., Honer, M., Becaud, J., Martic, M., Schubiger, P. A., Ametamey, S. M., et al. (2010) In vitro and in vivo characterization of novel ^{18}F-labeled bombesin analogues for targeting GRPR-positive tumors. *Bioconjugate Chem. 21*, 1864−71.
(32) Richter, S., Wuest, M., Krieger, S. S., Rogers, B. E., Friebe, M., Bergmann, R., and Wuest, F. (2013) Synthesis and radiopharmacological evaluation of a high-affinity and metabolically stabilized ^{18}F-labeled bombesin analogue for molecular imaging of gastrin-releasing peptide receptor-expressing prostate cancer. *Nucl. Med. Biol. 40*, 1025−34.
(33) Hultsch, C., Schottelius, M., Auernheimer, J., Alke, A., and Wester, H. J. (2009) 18)F-fluoroglucosylation of peptides, exemplified on cyclo(RGDfK). *Eur. J. Nucl. Med. Mol. Imaging 36*, 1469−74.
(34) Flavell, R. R., Kothari, P., Reed, B., Vallabhajosula, S., Goldsmith, S., Kreek, M. J., and Muir, T. W. (2011) Rapid F-18 labeling of peptides using aniline catalyzed oximation with [18F]FDG. *J. Nucl. Med. 52* (Suppl 1), 1498.
(35) Dirksen, A., Hackeng, T. M., and Dawson, P. E. (2006) Nucleophilic catalysis of oxime ligation. *Angew. Chem., Int. Ed 118*, 7743−7746.
(36) Cescato, R., Maina, T., Nock, B., Nikolopoulou, A., Charalambidis, D., Piccand, V., and Reubi, J. C. (2008) Bombesin receptor antagonists may be preferable to agonists for tumor targeting. *J. Nucl. Med. 49*, 318−26.
(37) Cescato, R., Waser, B., Fani, M., and Reubi, J. C. (2011) Evaluation of 177Lu-DOTA-sst2 antagonist versus 177Lu-DOTA-sst2 agonist binding in human cancers *in vitro*. *J. Nucl. Med. 52*, 1886−90.
(38) Varasteh, Z., Velikyan, I., Lindeberg, G., Sörensen, J., Larhed, M., Sandström, M., Selvaraju, R. K., Malmberg, J., Tolmachev, V., and Orlova, A. (2013) Synthesis and characterization of a high-affinity NOTA-conjugated bombesin antagonist for GRPR-targeted tumor imaging. *Bioconjugate Chem. 24* (7), 1144−53.
(39) Maschauer, S., Haubner, R., Kuwert, T., and Prante, O. (2014) (18)F-glyco-RGD peptides for PET imaging of integrin expression: efficient radiosynthesis by click chemistry and modulation of biodistribution by glycosylation. *Mol. Pharmaceutics 11* (2), 505−15.

DOI: 10.1021/bc500599m
Bioconjugate Chem. 2015, 26, 201−212

(40) Maeding, P., Fuechtner, F., and Wuest, F. (2005) Module-assisted synthesis of the bifunctional labelling agent N-succinimidyl 4-[(18)F]fluorobenzoate ([(18)F]SFB). *Appl. Radiat. Isot. 63*, 329−32.
(41) Hamacher, K., Coenen, H. H., and Stocklin, G. (1986) Efficient stereospecific synthesis of no-carrier-added 2-[18F]fluoro-2-deoxy-D-glucose using a aminopolyether supported nucleophilic substitution. *J. Nucl. Med. 27*, 235−38.
(42) Waterhouse, R. N. (2003) Determination of lipophilicity and its use as a predictor of blood-brain barrier penetration of molecular imaging agents. *Mol. Imaging Biol. 5*, 376−89.

DOI: 10.1021/bc500599m
Bioconjugate Chem. 2015, 26, 201−212